Monthly Notices of the ROYAL ASTRONOMICAL SOCIETY

MNRAS **518,** 636–641 (2023) https://doi.org/10.1093/mnras/stac2879
Advance Access publication 2022 October 10

Spectroscopy of TOI-1259B – an unpolluted white dwarf companion to an inflated warm Saturn

Evan Fitzmaurice,[1] David V. Martin ,[1,2★] Romy Rodríguez Martínez,[1] Patrick Vallely ,[1,3] Alexander P. Stephan ,[1,4] Kiersten M. Boley ,[1,3] Rick Pogge ,[1] Kareem El-Badry ,[5] Vedad Kunovac [4] and Amaury H. M. J. Triaud [5]

[1]*Department of Astronomy, The Ohio State University, 4055 McPherson Laboratory, Columbus, OH 43210, USA*
[2]*Center for Cosmology and AstroParticle Physics, The Ohio State University, Columbus, OH 43210, USA*
[3]*Center for Astrophysics | Harvard & Smithsonian, 60 Garden St, Cambridge, MA 02138, USA*
[4]*Lowell Observatory, 1400 W. Mars Hill Rd., Flagstaff, AZ 86001, USA*
[5]*School of Physics and Astronomy, University of Birmingham, Edgbaston, Birmingham B15 2TT, UK*

Accepted 2022 September 12. Received 2022 September 4; in original form 2022 June 16

ABSTRACT

TOI-1259 consists of a transiting exoplanet orbiting a main-sequence star, with a bound outer white dwarf (WDs) companion. Less than a dozen systems with this architecture are known. We conduct follow-up spectroscopy on the WD TOI-1259B using the Large Binocular Telescope to better characterize it. We observe only strong hydrogen lines, making TOI-1259B a DA WD. We see no evidence of heavy element pollution, which would have been evidence of planetary material around the WD. Such pollution is seen in $\sim 25-50$ per cent of WDs, but it is unknown if this rate is higher or lower in TOI-1259-like systems that contain a known planet. Our spectroscopy permits an improved WD age measurement of $4.05^{+1.00}_{-0.42}$ Gyr, which matches gyrochronology of the main-sequence star. This is the first of an expanded sample of similar binaries that will allow us to calibrate these dating methods and provide a new perspective on planets in binaries.

Key words: planets and satellites: formation – binaries: eclipsing – stars: individual: TOI-1259 – stars: low-mass – stars: rotation.

1 INTRODUCTION

Roughly 25−50 per cent of white dwarfs (WDs) have elements heavier than helium in their upper atmospheres (Zuckerman et al. 2010; Koester, Gänsicke & Farihi 2014), such as silicon, magnesium, iron, carbon, and oxygen. This 'pollution', is unexpected, as the high gravity of a WD should cause these metals to gravitationally settle into the interior quickly (time-scales of weeks to a few thousand year, Paquette et al. 1986). Unless our observations are unrealistically well timed, it is argued that this pollution must be constantly replenished (Aannestad et al. 1993; Koester 2009). Potential sources of replenishment include a disintegrating planet (Vanderburg et al. 2015a; Gänsicke et al. 2019; Buchan et al. 2022), a circumstellar disc (Farihi 2016) or the bombardment of planetesimals/asteroids (Petrovich & Muñoz 2017; Stephan, Naoz & Zuckerman 2017). Whilst the specific source of the pollution is unknown and likely varied, broadly speaking it is believed to be planetary (Veras 2021) and we even have direct evidence of WD accretion (Cunningham et al. 2022).

In this paper, we conduct spectroscopy of the WD TOI-1259B. The WD was both discovered and determined to be in a stellar binary by El-Badry et al. (2019). It is separated from the main-sequence K-dwarf TOI-1259A by 13.9 arcsec, which corresponds to a projected separation of 1648 au (Fig. 1). It was later found by Martin et al. (2021) that TOI-1259A hosts a transiting inflated warm Saturn ($a_p/R_\star = 12.3$, $M_p = 0.44 M_{Jup}$, $R_p = 1.02 R_{Jup}$).[1] Only about a dozen systems are known with a main-sequence star, an orbiting exoplanet and a bound WD companion. Only in a few of these cases does the planet transit (review in Martin et al. 2021). To our knowledge, only three of these WDs have received spectroscopy (WASP-98, Southworth et al. 2020; HD 27442, Chauvin et al. 2006; Mugrauer et al. 2007, and HD 107148 Mugrauer & Dinçel 2016), and no pollution has ever been detected (see Section 4.3).

There are two motivations for this paper. First, we are looking for pollution in the WD. Since this would be a proxy for a planet, and the WD is bound to a known exoplanet, this is a novel means of probing planets around both stars of a wide binary. Only two binaries are known where both stars individually[2] host a planet: WASP-94 (Neveu-VanMalle et al. 2014) and XO-2 (Damasso et al. 2015). There have been many studies on the effect of stellar multiplicity on planet occurrence rates (Roell et al. 2012; Martin, Mazeh & Fabrycky

★ E-mail: martin.4096@osu.edu
NASA Sagan Fellow.
NSF Graduate Fellow.

[1]Not to be confused with WD 1856 + 534, the only known case of a WD itself hosting a bonafide, intact transiting planet (Vanderburg et al. 2020).
[2]As opposed to circumbinary planets, where the tight inner binary collectively hosts an outer planet (review in Martin 2018).

2015; Kraus et al. 2016; Martin 2018), with planets being less likely in binaries tighter than ≈200 AU (Moe & Kratter 2019). However, such studies only concern planets around one of the stars, not both. Our second motivation is to spectroscopically characterize the WD such that we may better measure its age through the WD cooling time-scale. This may be compared to other age-dating methods of gyrochronology and isochrone fitting.

Our paper is structured as follows. Section 2 details the observations using the MODS spectrograph at the LBT. In Section 3 we characterize both the WD and the exoplanet host star. The results are discussed in Section 4 before concluding in Section 5.

2 OBSERVATIONS

The TOI-1259 system contains two stars: a 12.08-Vmag K-dwarf and a 19.23-Vmag WD, separated by 13.9 arcsec (SDSS image in Fig. 1). We obtained spectra with both using the Multi-Object Double Spectrographs (MODS; Pogge et al. 2010) mounted on the twin 8.4-m Large Binocular Telescope. All observations were performed in long-slit mode using a 0.6-arcsec slit, oriented such that only one of the two stars was inside the slit for a given observation. MODS uses a dichroic that splits the light into separately optimized red and blue channels at ∼5650 Å. For these observations, we used the G400L reflection grating on the blue channel and the G670L reflection grating on the red channel. The MODS blue channels cover a wavelength range of ∼3200−5650 Å with a resolution of R ∼ 1850 in the dual grating setup, while the MODS red channels cover ∼5650−9800 Å with a resolution of R ∼ 2300. The spectra were reduced using the MODSCCDRED (Pogge 2019)[3] PYTHON package for basic 2D CCD reductions, and the MODSIDL pipeline (Croxall & Pogge 2019)[4] to extract 1D spectra and apply wavelength and flux calibrations. Obserations were also taken of the exoplanet host star TOI-1259A. two sequences of five 120-s exposures. Ultimately, these were not used in any analysis.

For the host star TOI-1259A, we use existing SOPHIE spectra taken using the 1.93 m telescope at Observatoire de Haute Provence. Whilst it has significantly smaller (1.92 m) aperture than the LBT, the higher resolution of SOPHIE (R ∼40 000 in high-efficiency mode) is needed to characterize TOI-1259A's metallicity. The data are publicly available[5] and their acquisition is described in Martin et al. (2021).

3 ANALYSIS AND RESULTS

3.1 Exoplanet host star TOI-1259A parameters

We determine the stellar parameters of the host star using the publicly available EXOFASTv2 exoplanet suite (Eastman, Gaudi & Agol 2013; Eastman et al. 2019), which fits exoplanet data but has the capability of modeling stellar-only properties. We perform a spectral energy distribution (SED) fit of the star with the Kurucz (1992) atmosphere models and using broad-band photometry; specifically, we use the Gaia G, $G_{\rm BP}$, and $G_{\rm RP}$ magnitudes, *JHK* magnitudes from the 2MASS catalog (Cutri & et al. 2014), and the W1–W4 magnitudes from *WISE* (Zacharias et al. 2004). To independently derive an age of the system, we combine the SED fit with three different stellar evolutionary models within EXOFASTv2. We first derive an age using the MESA Isochrones and Stellar Tracks (MIST; Choi et al. 2016; Dotter 2016) isochrones, which assume a non-rotating star. We also perform fits using the Yonsei-Yale (YY) evolutionary tracks (Yi et al. 2001) and the PARSEC models (Bressan et al. 1993), which are similar to the MIST models.

For every fit, we impose initial guesses for the stellar mass $M_\star$, radius $R_\star$, and $T_{\rm eff}$ which are taken from the TESS Input Catalog (TIC-8; Stassun et al. 2019). We adopt a prior on the visual extinction A_V from the Schlegel dust maps (Schlegel, Finkbeiner & Davis 1998) and a parallax from the Gaia DR3 (Gaia Collaboration et al. 2020). Based on our isochrone fitting we obtain approximate stellar ages of 5 Gyr, with uncertainties on the order of a few Gyr. These are weak constraints in comparison to gyrochronology and WD cooling.

We determine the [Fe/H] metallicity of the host star from a high-resolution (R ∼39 000) optical spectrum from the SOPHIE spectrograph, which spans the wavelength range 3870−6944 nm. The spectrum we use has a signal-to-noise ratio of ∼20, which is the highest in our observations. We use the open-source framework for spectral analysis, `iSpec` (Blanco-Cuaresma et al. 2014; Blanco-Cuaresma 2019). `iSpec` calculates stellar atmospheric parameters as well as individual abundances using the synthetic spectral fitting method and the equivalent width method. For this target, we chose the synthetic spectral fitting method, as recommended by Blanco-Cuaresma et al. (2014). Within the `iSpec` framework, we employ the radiative transfer code SPECTRUM (Gray & Corbally 1994), the solar abundances from Grevesse, Asplund & Sauval (2007), the MARCS.GES atmosphere models (Gustafsson et al. 2008), and the atomic line list from the Gaia-ESO Survey (GES). The stellar parameters required for the abundance determinations, namely, the stellar effective temperature and surface gravity, were taken from our EXOFASTv2 analysis. These were $T_{\rm eff} = 4747^{+72}_{-74}$ K, and $\log g_* = 4.6 \pm 0.025$. We fix the limb-darkening coefficient to 0.6, and we fix the stellar rotation, $v \sin i_\star$, to 2 km s^{-1} (which is a typical value for sun-like stars) to avoid possible degeneracies between the macroturbulence and rotation, following the recommendations of Blanco-Cuaresma et al. (2014). We determine a final metallicity of [Fe/H] $= -0.1 \pm 0.04$ dex.

3.2 WD companion TOI-1259B parameters

The reduced one-dimensional spectrum of the WD is shown in the top right-hand panel of Fig. 1. Outlier data were removed by visual inspection. The light red bands indicate regions where telluric features are expected. Hydrogen features in the Balmer series that are present are labeled (H-α, -β, -γ, -δ, -ϵ). The spectrum lacks any features of helium or metals. Because of the presence of the hydrogen features and the absence of other lines, we classify this WD as a DA WD.

We use the open source package `wdtools` (Chandra et al. 2020),[6] which is designed to fit DA WD spectra and derive the effective temperature, $T_{\rm eff}$, and surface gravity, log$g$. This software interfaces with theoretical spectra computed by Tremblay & Bergeron (2009), Koester (2010). We use the Generative Fitting Pipeline (GFP) method. To build this method Chandra et al. (2020) use private state-of-the-art atmospheric models to create initial synthetic spectra and fit them to SDSS spectra. For computational efficiency, they use a neural network adapted for WD spectra to generate more synthetic

[3] https://github.com/rwpogge/modsCCDRed
[4] https://github.com/rwpogge/modsIDL
[5] The 'objname' in the SOPHIE database is GSC4591-0930. All spectra can be found here: http://atlas.obs-hp.fr/sophie/sophie.cgi?n=sophies&a=htab&ob=ra,seq&c=o&o = GSC4591-0930
[6] https://wdtools.readthedocs.io/

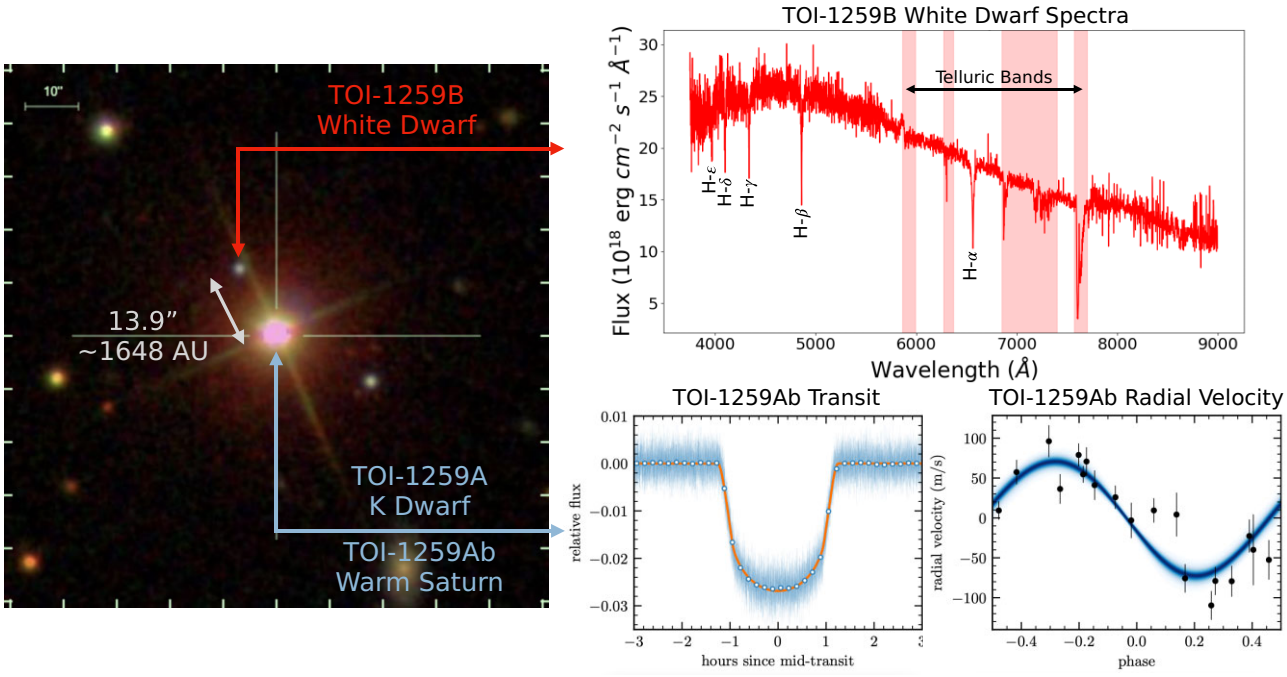

Figure 1. The TOI-1259 system, with a transiting warm Saturn and a bound WD companion. Left-hand panel: SDSS image showing the stellar binary. Top right-hand panel: One-dimensional reduced spectrum of the DA WD TOI-1259B. Outlier data was removed by visual inspection and manual cuts. Light red vertical bands are telluric absorption regions. Hydrogen features in the Balmer series are labeled. Bottom right- and left-hand panels**:** Phase folded and detrended TESS light curve of the transiting warm Saturn from Martin et al. (2021). Bottom right and right-hand panels**:** RV data of the warm Saturn from SOPHIE in black and 99th percentile models in the blue region from Martin et al. (2021).

spectra as a part of the fitting process. They reserve 1 per cent of their SDSS spectra for validation of the neural network model and obtain a relative error of less than 0.01 in normalized flux units across all pixels.

With the ability to generate unlimited high-quality synthetic spectra, they utilize an Markov chain Monte Carlo (MCMC) algorithm to sample the posterior and select the highest likelihood (lowest χ^2_r) fit for the labels of effective temperature and log$g$. The MCMC is able to take in a prior for the effective temperature in order to inform the fit.

We first scale the flux and flux errors by a factor of 10^{18} so that the program can accurately fit the continuum and normalize the spectrum. We inform the pipeline of the instrument spectral dispersion in angstroms. For MODS, this value is different for the red and blue channels that are used, being 0.8 and 0.5, respectively. We use an intermediate value of 0.65 since the data is combined in reduction. We inform the pipeline of the prior effective temperature of $T_{\rm eff} = 6300^{+80}_{-70}$ K that is derived from photometry in Martin et al. (2021). There is another prior from Mugrauer & Michel (2020) of $T_{\rm eff} = 6473^{+672}_{-419}$ K that we test but do not use as there is not a significant change in the produced values or fit. The pipeline allows for selection of specific hydrogen Balmer features to be used in the fit, so we elect to use the H-α, $-\beta$, $-\gamma$, $-\delta$, and $-\epsilon$ features since they are all present in the spectrum. The produced spectroscopic fit and labels are shown in Fig. 2. We derive an effective temperature of $T_{\rm eff} = 6612 \pm 23$ K, and a log$g = 8.42 \pm 0.03$.

For comparison, we re-create the SED fit of the WD by following Martin et al. (2021) but with two improvements. First, the biggest improvement is that we are now certain it is a DA, whereas previously there was a systematic uncertainty in the ages due to our ignorance of the WD spectral type. Secondly, we provide a metallicity prior

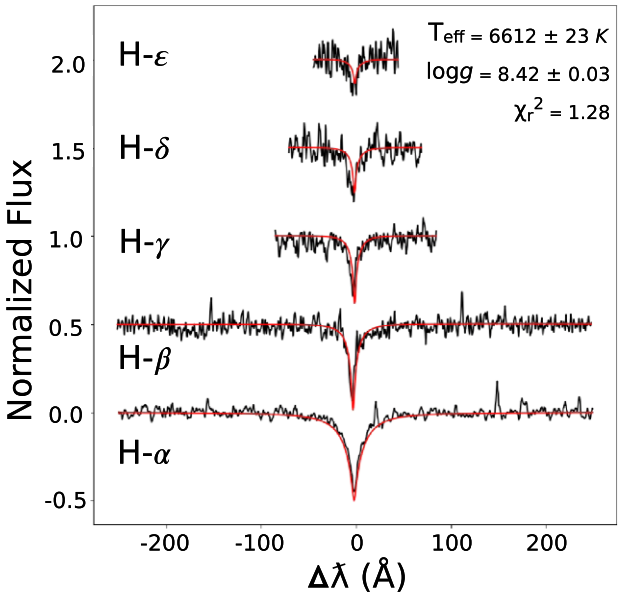

Figure 2. Spectroscopy of the DA WD TOI-1259B. We determine $T_{\rm eff}$ and log$g$ from fitting the H-α, $-\beta$, $-\gamma$, $-\delta$, and $-\epsilon$ lines using `wdtools` (Chandra et al. 2020).

of [Fe/H] $= -0.1 \pm 0.04$ dex based on spectroscopic analysis of the main-sequence TOI-1259A. This is an improvement on the rough [Fe/H] $= -0.2 \pm 0.3$ dex used in Martin et al. (2021), taken from the Tess Input Catalog (TIC). Like in Martin et al. (2021) we use two different WD Initial Final Mass Relations (IFMR): Williams, Bolte & Koester (2009) and El-Badry, Rix & Weisz (2018).

We derive an SED temperature of $T_{\rm eff} = 6330 \pm 70$ K, which differs slightly from the spectroscopic temperature of $T_{\rm eff} = 6612 \pm 23$ K. Typically, in the era of Gaia-derived distances the SED result should be considered more trustworthy. To first approximation, the SED just relies on the Stefan–Boltzmann law, whereas the interpretation of the WD spectrum relies on complicated non-local thermodynamic equilibrium radiative transfer calculations (Bergeron et al. 2019; Genest-Beaulieu & Bergeron 2019). Our age constraints are slightly tighter than in Martin et al. (2021), with $3.74^{+0.50}_{-0.22}$ using the Williams et al. (2009) and $4.05^{+1.00}_{-0.42}$ Gyr using El-Badry et al. (2018). The mass of the WD in these fits is $0.57 \pm 0.02\,{\rm M}_{\odot}$.

The constraints we derive on the WD's age represent formal fitting uncertainties, and do not account for systematics such as uncertainties in the WD-cooling models, uncertainties in the IFMR, or problems with the observational data. The fact that our inferred spectroscopic and photometric temperatures for the WD are formally inconsistent suggests that the errors on both quantities could be underestimated. We performed two-fitting experiments to assess the effects of systematics and underestimated uncertainties on our age constraints.

First, we tried inflating the SDSS photometric uncertainties until our photometric and spectroscopic temperature constraints were consistent. We found that this was achieved when we inflated the uncertainty in all bands to 0.08 mag (where the reported values are ∼0.02 mag). Re-running BASE-9 with these inflated uncertainties and the El-Badry et al. (2018) IFMR, we found a photometric temperature of 6459 ± 140 K, which is consistent within 1σ with the spectroscopic value. In this case, the inferred total age changes from $4.05^{+1.00}_{-0.42}$ to $3.62^{+1.52}_{-0.30}$ Gyr. As expected, this value is consistent with what we inferred from the reported uncertainties but has a somewhat larger errorbar.

Next, we removed the photometry from the fit and instead put a tight prior on the WD temperature and surface gravity from our spectroscopic fit. In this case, we obtained a total age of $3.01^{+0.32}_{-0.09}$ Gyr, which is inconsistent at the $\sim 2\sigma$ level with our nominal uncertainty. This is not surprising, since the photometric and spectroscopic effective temperatures differ at the $\sim 3\sigma$ level.

In summary, all the WD age-fitting approaches, we explored place it an an age between about 2.9 and 5 Gyr. The differences between ages inferred under different assumptions are comparable to the formal fitting uncertainty under our fiducial assumptions, and thus do contribute to to the total realistic uncertainty budget. This is not unexpected for a relatively low-mass WD such as TOI-1259B, for a small change in inferred age can translate to a significant change in both cooling and pre-WD age (e.g. Heintz et al. 2022).

4 DISCUSSION

4.1 Comparative age measurements

Table 1 shows the age constraints from the three isochrones tested (Section 3.1), the WD-cooling age (Section 3.2), and gyrochronology age derived in Martin et al. (2021). The gyrochronological age, which we do not recalculate here, is based on a Systematics-Insensitive Periodogram from Hedges et al. (2020) where astrophysical periodicities in the light curve are isolated with respect to background variations due to the spacecraft. This rotation rate is converted into an age following the methodology of Angus et al. (2020).

For the WD ages there are two components: the time spent as a WD (the cooling time) and the time spent before becoming a WD (essentially its main-sequence age). The cooling age is very well constrained: $1.89^{+0.07}_{-0.06}$ Gyr. The pre-WD age is much less certain because the time a star spends on the main sequence is a sensitive function of stellar mass, and we have to estimate the main-sequence progenitor's mass based on the current WD mass. This process also suffers from a systematic uncertainty related to the choice of the IFMR (Williams et al. 2009 or El-Badry et al. 2018), which is why we provide both ages in Table 1.

Table 1. Age measurements for the TOI-1259 based on different methods.

Method	Age (Gyr)	Error (Gyr)
1. Isochrone (MIST)	4.9	$^{+5.5}_{-3.5}$
2. Isochrone (Yonsei-Yale)	5.3	$^{+4.8}_{-3.7}$
3. Isochrone (PARSEC)	5.2	$^{+5.2}_{-3.7}$
4. WD Cooling (Williams et al. 2009 IFMR)	3.74	$^{+0.50}_{-0.22}$
5. WD Cooling (El-Badry et al. 2018 IFMR)	4.05	$^{+1.00}_{-0.42}$
6. Gyrochronology	4.8	$^{+0.7}_{-0.8}$

Our WD age measurements are improved in comparison with Martin et al. (2021) in two ways. First, the by confirming TOI-1259B as a DA WD we have removed a large source of systematic uncertainty of the WD spectral type. This uncertainty propagates into the stellar parameters and ultimately the age. The second improvement comes from better constraining the metallicity of the WD progenitor, since main-sequence age is also affected by metallicity. This comes through spectral characterisation of the main-sequence TOI-1259A, which we presume has the same metallicity. Overall, we have a ∼ 20 per cent tighter age constraint than Martin et al. (2021).

For completeness, we include in Table 1 the stellar ages derived from our isochrone fits to the primary star TOI-1259A (MIST, Yonsei-Yale and PARSEC). However, given the low mass ($M_{\rm A} = 0.744\,{\rm M}_{\odot}$) and hence long expected lifetime for this K-dwarf, the isochrones provide very little constraint on its age, as reflected in the large errorbars. The gyrochronology and WD cooling ages are much more constraining, with $\delta t_{\rm Age} \approx 20$ per cent, and it is re-assuring to see that these two methods match. An expanded sample of WD + main-sequence binaries will provide a more thorough comparison and calibration of these two age dating methods.

4.2 Lack of pollution in context of TOI-1259's dynamical history

Zuckerman (2014) determined that the rate of WD pollution was the same in single WDs as in WDs in wide (>1000 au) binaries. For tighter binaries the WD pollution rate was decreased. This may indicate that in these tighter binaries planet formation is suppressed due to binary interactions. This matches exoplanets in main-sequence binaries both in terms of observations (Kraus et al. 2016; Su et al. 2021) and theory (Kley & Nelson 2008; Marzari & Thebault 2019). However, in the Zuckerman (2014) sample the main-sequence star in the binary was not known to host a planet. It is unknown what the pollution rate is in TOI-1259-like architectures.

Whilst the WD spectrum produced from our observations shows no signs of such pollution in TOI-1259B, the absence of such lines does not conclusively rule out that this WD has not ever had planets or has not ever been polluted by planetary material in the past. Specifically, given the age and architecture of the TOI-1259 system, a variety of scenarios may explain the current absence of metal lines, while still allowing for frequent pollution events.

For example, the presence of the stellar companion may have driven most planetary material into the WD progenitor during the main-sequence and red giant phases via the Kozai–Lidov mechanism (Kozai 1962; Lidov 1962; Martin & Triaud 2016; Naoz 2016), with only a small amount of material available for accretion for the WD (a scenario discussed in Stephan et al. 2017). These pollution events may also only occur sporadically, with accreted material quickly settling into the deeper WD layers, avoiding detection. For our WD, we expect a settling time-scale of ≈5000−10 000 years, which is much shorter than the cooling time-scale (Paquette et al. 1986; Bédard et al. 2020). As the Kozai–Lidov mechanism is only effective on bodies in specific parts of the eccentricity-inclination parameter space, there may also still be significant amounts of planetary material left on orbits that do not allow them to come close to the WD.

In order to determine if the presence of a stellar companion aids or hinders to pollute WDs with planetary material, a larger sample of WDs in binaries will have to be observed to allow comparisons with the expected value of 25−50 per cent from single WD observations.

4.3 Comparison with other WDs in binaries

Previous works have performed similar analysis on the spectroscopy and photometry of WD companions to exoplanet hosting stars. Southworth et al. (2020) analyzed the spectra of the WD WASP-98B and found a featureless spectrum which prohibited a precise age estimation. Mugrauer & Dinçel (2016) analyzed the spectra of HD 107148B and determined a spectral-type DA. The effective temperature was found to be between 5900 and 6400 K, and they deduced a total age of the system to be 6.0 ± 4.8 Gyr. Mugrauer and Neuhäuser et al. (2007) and Chauvin et al. (2006) both analyzed the WD companion HD 27442B. This WD is classified as a DA WD with an effective temperature ∼14400 K and a cooling age of ∼220 Myr, but a total age is not computed. Vanderburg et al. (2015b) did photometric analysis of HIP 116454B using SDSS *ugriz* data and determined an effective temperature of 7500 ± 200 K and cooling age of ∼1.3 Gyr. TOI-1259 stands out in this sample in that not only do we have a WD cooling age but we also have a gyrochronology age.

Stellar age calibration for WD-MS binaries has been applied for many different scenarios. Catalán et al. (2008), Cummings et al. (2018), and Williams et al. (2009) use WDs in binaries to refine initial–final mass relations by using spectroscopic and photometric measurements of the WD and its companion to determine the WD cooling age, as well as the progenitor mass as determined from the estimated age of the main-sequence companion. Fouesneau et al. (2019) and Qiu et al. (2021) pair spectroscopic and distance measurements to determine ages of field stars with WD companions that are otherwise difficult to determine. Rebassa-Mansergas et al. (2021) uses this method to refine age measurements of stars in the solar neighborhood to determine the age–metallicity relation. Garcés, Catalán & Ribas (2011) tracks the decrease in high-energy emission of low mass stars by using WD companions to calibrate the ages. This method of age calibration using WD companions is broadly applicable and widely trusted, and serves as a reliable mechanism for our purpose.

5 CONCLUSION

We use the MODS spectrograph on the LBT to observe the WD TOI-1259B, which is a bound companion to the inflated warm Saturn TOI-1259b. We observe solely strong Hydrogen lines, characterizing it as a DA WD. No heavy element pollution is seen in the WD's atmosphere, which would have been evidence of planets (or at least planetary material) around both stars in a wide binary, a phenomena for which there exists only minimal observational constraints. Whilst WD pollution is seen in roughly 25−50 per cent of single WDs (Zuckerman et al. 2010; Koester et al. 2014), and similarly in >1000 binaries (Zuckerman 2014), we have no constraints on the rate of WD pollution in TOI-1259-like architectures where the main-sequence star hosts a planet.

The TOI-1259 system remains interesting for future follow-up. As an inflated warm Saturn ($a_p/R_\star = 12.3$, $M_p = 0.44 M_{Jup}$, $R_p = 1.02 R_{Jup}$) with very deep 2.7 per cent transits around a K-dwarf it is an ideal target for atmospheric characterisation (Kempton et al. 2018). Unlike most exoplanets, the WD companion provides a reliable and precise (∼ 20 per cent) age measurement. Therefore, any future observations that would speak to a dynamical past, such as companion planets, spin–orbit obliquities or residual eccentricity, could be better interpreted.

ACKNOWLEDGEMENTS

We thank an anonymous referee for a thorough report which definitely improved the quality of this paper.

This paper made use of data obtained with the Large Binocular Telescope (LBT). The LBT is an international collaboration among institutions in the United States, Italy and Germany. LBT Corporation partners are: The University of Arizona on behalf of the Arizona Board of Regents; Istituto Nazionale di Astrofisica, Italy; LBT Beteiligungsgesellschaft, Germany, representing the Max-Planck Society, The Leibniz Institute for Astrophysics Potsdam, and Heidelberg University; The Ohio State University, representing OSU, University of Notre Dame, University of Minnesota and University of Virginia.

LBT MODS data in this paper used the modsIDL spectral data reduction pipeline and the modsCCDRed data reduction code developed in part with funds provided by NSF Grants AST-9987045 and AST-1108693, and a gift from David G. Price through the Price Fellowship in Astronomical Instrumentation.

This project used funding from the NASA TESS Guest Investigator Program (G04157, PI Martin). Support for DVM's work was provided by NASA through the NASA Hubble Fellowship grant HF2-51464 awarded by the Space Telescope Science Institute, which is operated by the Association of Universities for Research in Astronomy, Inc., for NASA, under contract NAS5-26555. V.K. acknowledges support from NSF award AST2009501.

DATA AVAILABILITY

The SOPHIE and MODS spectroscopy will be made publicly available. Any data fits can be provided on request to the authors.

REFERENCES

Aannestad P. A., Kenyon S. J., Hammond G. L., Sion E. M., 1993, AJ, 105, 1033
Angus R. et al., 2020, AJ, 160, 90
Bédard A., Bergeron P., Brassard P., Fontaine G., 2020, ApJ, 901, 93
Bergeron P., Dufour P., Fontaine G., Coutu S., Blouin S., Genest-Beaulieu C., Bédard A., Rolland B., 2019, ApJ, 876, 67
Blanco-Cuaresma S., 2019, MNRAS, 486, 2075
Blanco-Cuaresma S., Soubiran C., Heiter U., Jofré P., 2014, A&A, 569, A111
Bressan A., Fagotto F., Bertelli G., Chiosi C., 1993, A&AS, 100, 647

Buchan A. M., Bonsor A., Shorttle O., Wade J., Harrison J., Noack L., Koester D., 2022, MNRAS, 510, 3512
Catalán S., Isern J., García-Berro E., Ribas I., Allende Prieto C., Bonanos A. Z., 2008, A&A, 477, 213
Chandra V., Hwang H.-C., Zakamska N. L., Budavári T., 2020, MNRAS, 497, 2688
Chauvin G., Lagrange A.-M. Udry S., Fusco T. Galland F., Naef D. Beuzit J.-L., Mayor M., 2006, A&A, 456, 1165
Choi J., Dotter A., Conroy C., Cantiello M., Paxton B., Johnson B. D., 2016, ApJ, 823, 102
Croxall K. V., Pogge R. W., 2019, rwpogge/modsIDL: modsIDL Binocular Release
Cummings J. D., Kalirai J. S., Tremblay P. E., Ramirez-Ruiz E., Choi J., 2018, ApJ, 866, 21
Cunningham T., Wheatley P. J., Tremblay P.-E., Gänsicke B. T., King G. W., Toloza O., Veras D., 2022, Nature, 602, 219
Cutri R. M., et al., 2014, VizieR Online Data Catalog, 2328
Damasso M. et al. 2015, A&A, 575, A111
Dotter A., 2016, ApJS, 222, 8
Eastman J., Gaudi B. S., Agol E., 2013, Publ. Astron. Soc. Pac., 125, 83
Eastman J. D. et al. 2019, preprint (arXiv:1907.09480)
El-Badry K., Rix H.-W., Weisz D. R., 2018, ApJ, 860, L17
El-Badry K., Rix H.-W., Tian H., Duchêne G., Moe M., 2019, MNRAS, 489, 5822
Farihi J., 2016, New Astron Rev, 71, 9
Fouesneau M., Rix H.-W., von Hippel T., Hogg D. W., Tian H., 2019, ApJ, 870, 9
Gaia Collaboration, Brown A. G. A., Vallenari A., Prusti T., de Bruijne J. H. J., Babusiaux C., Biermann M., 2020, A&A, 649, 20
Gänsicke B. T., Schreiber M. R., Toloza O., Gentile Fusillo N. P., Koester D., Manser C. J., 2019, Nature, 576, 61
Garcés A., Catalán S., Ribas I., 2011, A&A, 531, A7
Genest-Beaulieu C., Bergeron P., 2019, ApJ, 871, 169
Gray R. O., Corbally C. J., 1994, AJ, 107, 742
Grevesse N., Asplund M., Sauval A. J., 2007, Space Sci. Rev., 130, 105
Gustafsson B., Edvardsson B., Eriksson K., Jørgensen U. G., Nordlund, Å., Plez B., 2008, A&A, 486, 951
Hedges C., Angus R., Barentsen G., Saunders N., Montet B. T., Gully-Santiago M., 2020, Res Notes AAS, 4, 220
Heintz T. M., Hermes J. J., El-Badry K., Walsh C., van Saders J. L., Fields C. E., Koester D., 2022, ApJ, 934, 17
Kempton E. M.-R. et al. 2018, Publ. Astron. Soc. Pac., 130, 114401
Kley W., Nelson R. P., 2008, A&A, 486, 617
Koester D., 2009, A&A, 498, 517
Koester D., 2010, Mem. Soc. Astron. Ital., 81, 921
Koester D., Gänsicke B. T., Farihi J., 2014, A&A, 566, A34
Kozai Y., 1962, AJ, 67, 591
Kraus A. L., Ireland M. J., Huber D., Mann A. W., Dupuy T. J., 2016, AJ, 152, 8
Kurucz R. L., 1992, in Barbuy B., Renzini A., eds, IAU Symp. Vol. 149, The Stellar Populations of Galaxies. Kluwer, Dordrecht. p. 225
Lidov M. L., 1962, Planet. Space Sci., 9, 719
Martin D. V. et al., 2021, MNRAS, 507, 4132
Martin D. V., 2018, Populations of Planets in Multiple Star Systems. Springer International Publishing, Cham, p. 2035
Martin D. V., Triaud A. H. M. J., 2016, MNRAS, 455, L46
Martin D. V., Mazeh T., Fabrycky D. C., 2015, MNRAS, 453, 3554
Marzari F., Thebault P., 2019, Galaxies, 7, 84
Moe M., Kratter K. M., 2019, MNRAS, 507, 3593
Mugrauer M., Dinçel B., 2016, Astron. Nachr., 337, 627
Mugrauer M., Michel K. U., 2020, Astron. Nachr., 341,996
Mugrauer M., Neuhäuser R. Mazeh T., 2007, A&A, 469, 755
Naoz S., 2016, ARA&A, 54, 441
Neveu-VanMalle M. et al., 2014, A&A, 572, A49
Paquette C., Pelletier C., Fontaine G., Michaud G., 1986, ApJS, 61, 197
Petrovich C., Muñoz D. J., 2017, ApJ, 834, 116
Pogge R., 2019, rwpogge/modsCCDRed: v2.0.1,
Pogge R. W. et al., 2010, Ground-based and Airborne Instrumentation for Astronomy III. SPIE, Bellingham, WA, USA, p. 77350A
Qiu D., Tian H.-J., Wang X.-D., Nie J.-L., von Hippel T., Liu G.-C., Fouesneau M., Rix H.-W., 2021, ApJS, 253, 58
Rebassa-Mansergas A. et al., 2021, MNRAS, 505, 3165
Roell T., Neuhäuser R., Seifahrt A., Mugrauer M., 2012, A&A, 542, A92
Schlegel D. J., Finkbeiner D. P., Davis M., 1998, ApJ, 500, 525
Southworth J., Tremblay P.-E., Gänsicke B. T., Evans D., Močnik T., 2020, MNRAS, 497, 4416
Stassun K. G. et al., 2019, AJ, 158, 138
Stephan A. P., Naoz S., Zuckerman B., 2017, ApJ, 844, L16
Su X.-N., Xie J.-W., Zhou J.-L., Thebault P., 2021, AJ, 162, 272
Tremblay P. E., Bergeron P., 2009, ApJ, 696, 1755
Vanderburg A. et al., 2015a, Nature, 526, 546
Vanderburg A. et al., 2015b, ApJ, 800, 59
Vanderburg A. et al., 2020, Nature, 585, 363
Veras D., 2021, Oxford Research Encyclopedia of Planetary Science. Oxford University Press, York, NY, USA, p. 1
Williams K. A., Bolte M., Koester D., 2009, ApJ, 693, 355
Yi S., Demarque P., Kim Y.-C., Lee Y.-W., Ree C. H., Lejeune T., Barnes S., 2001, ApJS, 136, 417
Zacharias N., Monet D. G., Levine S. E., Urban S. E., Gaume R., Wycoff G. L., 2004, American Astronomical Society Meeting Abstracts. p. 1418
Zuckerman B., 2014, ApJ, 791, L27
Zuckerman B., Melis C., Klein B., Koester D., Jura M., 2010, ApJ, 722, 725

SUPPORTING INFORMATION

Supplementary data are available at *MNRAS* online.

Please note: Oxford University Press is not responsible for the content or functionality of any supporting materials supplied by the authors. Any queries (other than missing material) should be directed to the corresponding author for the article.

This paper has been typeset from a TEX/LATEX file prepared by the author.